BIOCHEMISTRY
including biophysical chemistry & molecular biology

Article

pubs.acs.org/biochemistry

H Atom Positions and Nuclear Magnetic Resonance Chemical Shifts of Short H Bonds in Photoactive Yellow Protein

Keisuke Saito[†] and Hiroshi Ishikita*[,†,‡]

[†]202 Building E, Career-Path Promotion Unit for Young Life Scientists, Graduate School of Medicine, Kyoto University, Yoshida-Konoe-cho, Sakyo-ku, Kyoto 606-8501, Japan

[‡]Japan Science and Technology Agency (JST), PRESTO, 4-1-8 Honcho Kawaguchi, Saitama 332-0012, Japan

Supporting Information

ABSTRACT: Recent neutron diffraction studies on photoactive yellow protein (PYP) proposed that the H bond between protonated Glu46 and the chromophore-ionized *p*-coumaric acid (*p*CA) is a low-barrier H bond (LBHB) mainly because the H atom position was assigned at the midpoint of the O_{Glu46}–O_{pCA} bond. However, the ^{1}H nuclear magnetic resonance (NMR) chemical shift (δ_H) was 15.2 ppm, which is lower than the values of 17–19 ppm for typical LBHBs. We evaluated the dependence of δ_H on an H atom position in the O_{Glu46}–O_{pCA} bond in the PYP ground state by using a quantum mechanical/molecular mechanical (QM/MM) approach. The calculated chemical shift unambiguously suggested that a δ_H of 15.2 ppm for the O_{Glu46}–O_{pCA} bond in NMR studies should correspond to the QM/MM geometry (δ_H = 14.5 ppm), where the H atom belongs to the Glu moiety, rather than the neutron diffraction geometry (δ_H = 19.7 ppm), where the H atom is near the midpoint of the donor and acceptor atoms.

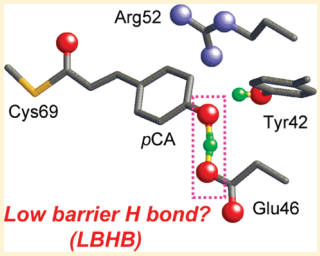

Photoactive yellow protein (PYP) serves as a bacterial photoreceptor, in particular, as a sensor for negative phototaxis to blue light.[1] The photoactive chromophore of PYP is *p*-coumaric acid (*p*CA), which is covalently attached to Cys69.[2] In the PYP ground state, the *p*CA chromophore exists as a phenolate anion.[3−5] The PYP crystal structure revealed that *p*CA is H-bonded by protonated Tyr42 and protonated Glu46 (Figure 1). Tyr42 is further H-bonded by Thr50. Structural analysis suggested that Glu46 is protonated and *p*CA is ionized in the PYP ground state, pG.[6,7]

Recently, hydrogen or deuterium atom positions of PYP were assigned via neutron diffraction analysis.[8] [Note that both hydrogen (H) and deuterium (D) are termed H atoms in our study. Changes in the H bond donor–acceptor distances due to H–D substitution are negligible; for instance, it is found to be 0.01 Å in NMR studies on PYP.[9]] According to neutron diffraction analysis, in the case of the Glu46–*p*CA pair, an H atom was 1.21 Å from Glu46 and 1.37 Å from *p*CA, almost at the midpoint of the O_{Glu46}–O_{pCA} bond (2.57 Å) (Figure 1a). From this unusual H atom position, the H bond between Glu46 and *p*CA was interpreted as a low-barrier H bond (LBHB[10]) in ref 8.

An LBHB is a nonstandard H bond, which was originally proposed to possess a covalent bond-like character, thus significantly stabilizing the transition state and facilitating enzymatic reactions.[10,11] In original reports by Frey et al.[11] or Cleland and Kreevoy,[10] it was stated that an LBHB forms when the pK_a difference between donor and acceptor moieties is nearly zero. If this is the case, the identification of an LBHB with a single minimum potential can be valid only if the minimum is at the center of the O_{Glu46}–O_{pCA} bond (i.e., the pK_a values of the two moieties are nearly equal), as suggested by Schutz and Warshel.[12] The H atom position in the O_{Glu46}–O_{pCA} bond in the neutron diffraction study appears to satisfy the criterion of an LBHB, which should yield the similar pK_a values for Glu46 and *p*CA. However,

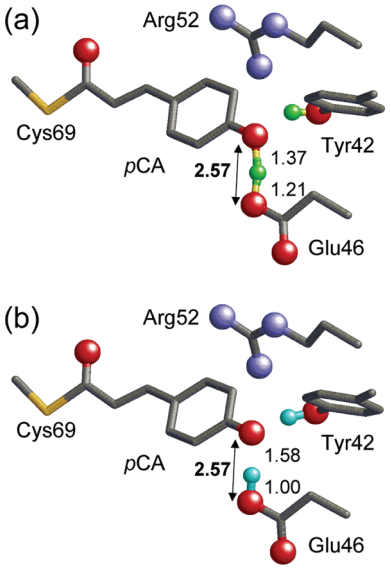

Figure 1. Geometry of the photoactive site in PYP. Only the H atom position of the H bonds between Tyr42 and *p*CA and between Glu46 and *p*CA are shown (green or cyan spheres). Oxygen and nitrogen atoms of the side chains are depicted as red and blue spheres, respectively. (a) Neutron diffraction analysis (PDB entry 2ZOI). (b) QM/MM-optimized structure based on the X-ray crystal structure (PDB entry 2ZOH).

Received: December 19, 2011
Revised: January 13, 2012
Published: January 20, 2012

the "similar pK_a values of Glu46 and *p*CA" contradict the protonated Glu46 and deprotonated *p*CA in the PYP ground state, as suggested in a number of previous experimental studies.[3−5,13] The negative bands at 1740 (78 K) and 1736 cm^{-1} (250 K) in FTIR studies were due to the C═O stretch of protonated Glu46 in the PYP ground state, suggesting that Glu46 is protonated in the presence of ionized *p*CA.[13]

In the previous study, we calculated pK_a(Glu46) and pK_a(*p*CA) by using the 1.25 Å structure (PDB entry 2ZOH[8]) and by solving the linear Poisson−Boltzmann equation with consideration of the protonation states of all titratable sites in the entire PYP.[14] In contrast to the pK_a values of 4.4 for Glu[15] and 8.8 for *p*CA[16] in aqueous solution, the calculated values of pK_a(Glu46) (∼9) and pK_a(*p*CA) (∼6)[14] support the previous results[3−5,13] [e.g., Tyr42 is an H bond donor of *p*CA, stabilizing ionized *p*CA and decreasing pK_a(*p*CA) by ∼2 units; the downshift in pK_a(*p*CA) simultaneously upshifts the pK_a of the H bond partner, Glu46[14]]. This also suggests that the energetics deduced from the heavy atom positions of the crystal structure (PDB entry 2ZOH) are quite reasonable for reproducing the pK_a values.

It was suggested that a stronger H bond results in a more downfield ^{1}H NMR chemical shift. According to the classification of H bonds by Jeffrey[17] or Frey,[18] "single-well H bonds" are very short, typically with O−O distances of 2.4−2.5 Å, and display ^{1}H NMR chemical shifts (δ_H) of 20−22 ppm.[18] "LBHBs" are longer, 2.5−2.6 Å, with a δ_H of 17−19 ppm.[18] "Weak H bonds" are even longer, with a δ_H of 10−12 ppm.[18] According to the criteria provided in refs 18 and 19, the O_{Glu46}−O_{pCA} bond is not an LBHB but is more likely to be a single-well H bond in terms of the H atom position. However, the reported O_{Glu46}−O_{pCA} distance, 2.57 Å,[8] is too long for a single-well H bond. Thus, on the basis of the H bond geometry, it is unclear whether this protein has an LBHB. On the other hand, a δ_H of 15.2 ppm was assigned to protonated Glu46 in NMR studies.[9] The value of 15.2 ppm is smaller than that for single-well H bonds (20−22 ppm[18]) or even for an LBHB (17−19 ppm[18]). Furthermore, using a quantum mechanical/molecular mechanical (QM/MM) approach, we reproduced the short H bond distance of the crystal structure, Glu46−*p*CA (2.57 Å). However, the H atom obviously belonged to the Glu moiety,[14] in agreement with FTIR studies by Kandori et al.[13] Note that the O_{Glu46}−H−O_{pCA} angles were 167.9° in the neutron diffraction studies[8] (Figure 1a) and 169.7° in the QM/MM geometry[14] (Figure 1b), being essentially the same.

Although NMR studies and QM/MM studies indicated the same tendency, the actual H atom position that corresponds to a δ_H of 15.2 ppm in the O_{Glu46}−O_{pCA} bond is yet unclear. Because the type of H bond should not be classified on the basis of only a single conformation with regard to the H atom position (although it was done in ref 8), we reported not only (i) the geometry but also (ii) the potential energy profile of the H bond, (iii) pK_a values of the donor and acceptor moieties, and (iv) the protonation state of Arg52, which had been proposed to be deprotonated[8] to support the LBHB.[14] In this study, we further report a H atom position in the O_{Glu46}−O_{pCA} bond and the corresponding chemical shift. We calculated δ_H for the O_{Glu46}−O_{pCA} bond quantum chemically, with the full account of the complete PYP atomic coordinates, defining the *p*CA with the covalently bonded Cys69 and all H bond partner residues, i.e., Tyr42, Glu46, and Thr50, as the QM region and the remaining residues as the MM region.

COMPUTATIONAL PROCEDURES

As demonstrated in the previous article,[14] we employed the following systematic modeling procedure. First, we constructed a realistic molecular model of the whole PYP using the recently determined high-resolution crystal structure. Second, to gain a better understanding of the electronic structure of the chromophore *p*CA, and the residues in the H bond network, namely, Tyr42, Glu46, Thr50, and Cys69, we performed large-scale QM/MM calculations for the entire PYP protein. Technical details of each modeling procedure are summarized below.

The atomic coordinates were taken from the X-ray structures of PYP at 1.25 Å resolution (PDB entry 2ZOH)[8] and 1.10 Å resolution (PDB entry 1OTB).[20] We employed the so-called electrostatic embedding QM/MM scheme[21] and used the Qsite[22] program code that was as used in previous studies.[14] The detailed geometry of the QM region was optimized under the influence of MM electrostatic/steric field (see Table S1 of the Supporting Information for geometry and atomic charges). We employed the restricted DFT method with the B3LYP functional and LACVP**+ basis sets. The NMR chemical shift was calculated by using the GIAOs method[23] implemented in Qsite[22] and JAGUAR.[24] The absolute shielding constant of ^{1}H of tetramethylsilane (TMS) was calculated to be 31.6 ppm on the basis of the atomic coordinates in ref 25 and used as the TMS reference for δ_H. We optimized the geometries of maleate and compounds **1**−**4** at the B3LYP/LACVP**+ level. These calculations were performed with JAGUAR[24] (see Table S2 of the Supporting Information for the geometry). Further detailed analysis, e.g., reliable QM/MM calculations involving extensive sampling,[26] may be needed for scrutiny of this issue.

The calculated OHO bond geometries and the NMR chemical shifts were also evaluated by the correlation proposed by Limbach et al.[27] The geometric correlation of the $O_{acceptor}$···H−O_{donor} bond between the acceptor···hydrogen ($O_{acceptor}$···H) distance (r_1) and the donor−hydrogen (O_{donor}−H) distance (r_2) was obtained by

$$q_2 = 2r^0 + 2q_1 + 2b \ln[1 + \exp(-2q_1/b)]$$
$$b = [2\, q_{2\min} - 2\, r^0]/2\ln 2$$
$$q_1 = (r_1 - r_2)/2$$
$$q_2 = r_1 + r_2 \quad (1)$$

where $q_{2\,min}$ represents a minimum value corresponding to the minimum $O_{acceptor}$···O_{donor} distance in the case of a linear H bond and r^0 is the equilibrium distance in the fictive free diatomic unit OH.[27]

The correlation between the OHO bond geometry and the ^{1}H NMR chemical shift δ_H was obtained by

$$\delta_H = \delta_{OH}{}^0 + \Delta_H(4p_1p_2)^m$$
$$p_1 = \exp[-(q_1 + q_2/2 - r^0)/b]$$
$$p_2 = \exp[-(-q_1 + q_2/2 - r^0)/b] \quad (2)$$

where $\delta_{OH}{}^0$ and Δ_H represent the limiting chemical shifts of the separate fictive groups OH and the excess chemical shift of the quasi-symmetric complex, respectively, and m is an empirical parameter. q_2 is given in eq 1. We used the same parameters

that were used in ref 27, i.e., r^0 = 0.96 and $q_{2\ min}$ = 2.38 for Figure 3, and r^0 = 0.93, $q_{2\ min}$ = 2.36, $\delta_{OH}{}^0$ = 7.9, and Δ_H =13 for Figure 6 (note that in ref 27 we regarded lines 1−3 of Figure 5a as lines 3, 1, and 2 of Table 1).

RESULTS AND DISCUSSION

δ_H Values for Compounds. To evaluate the accuracy of the quantum chemically calculated δ_H, first we calculated δ_H for malaete and compounds **1**−**4** (Figure 2), which are supposed

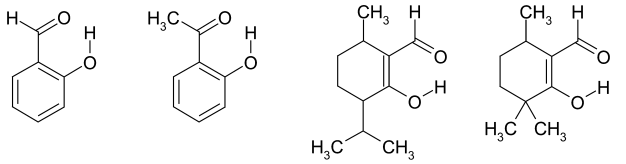

1 **2** **3** **4**

Figure 2. Compounds listed in Table 1.

to contain a "strong" H bond or an LBHB.[28] The calculated δ_H values are considerably close to the experimentally measured values, with discrepancies of approximately ≤1 ppm (Table 1).

Table 1. Experimental[28] and Calculated Values of δ_H (parts per million) for Compounds

	exptl δ_H	calcd δ_H
maleate	21.5	21.8
1	11.0	12.1
2	12.2	13.1
3	14.9	15.7
4	15.6	15.9

The discrepancy between the measured values (solution) and the calculated values (solid state) is mainly due to an insufficient account of the multiconfiguration of the molecular geometry, the proton dynamics, and the ro-vibrational corrections to the nuclear shielding in the calculations. In turn, this indicates that the contributions of these features to the values are obviously negligible, which does not practically affect any conclusions of this study. Hence, the calculated δ_H values should be considered at this accuracy level.

To quantitatively check the obtained H bond geometries, we investigated the "H bond correlation" previously established not only for solids but also for liquids by Steiner[29] or Limbach et al.[27] by defining r_1 and r_2 as acceptor···hydrogen ($O_{acceptor}$···H) and donor−hydrogen (O_{donor}−H) distances in the $O_{acceptor}$···H−O_{donor} bond, respectively ($r_1 > r_2$). Interestingly, the obtained H bond geometries of all compounds and PYP fitted exactly the proposed correlation curve (eq 1)[27] (Figure 3), demonstrating that the correlation in ref 27 reproduces the quantum chemically optimized $O_{acceptor}$···H and O_{donor}−H distances reasonably once the $O_{acceptor}$−O_{donor} distance is specified. In contrast, the H bond geometries of the neutron diffraction study[8] did not fit the proposed correlation curve. Possibly, the deviation may be associated with thermal ellipsoids arising from nonresolved half-protons on both sides of the H bond center and/or thermal motions,[27,29] in particular when two tautomeric forms are present.[30]

δ_H for PYP. Using the QM/MM-optimized geometry, we calculated the δ_H values for the O_{Glu46}−O_{pCA} and O_{Tyr42}−O_{pCA}

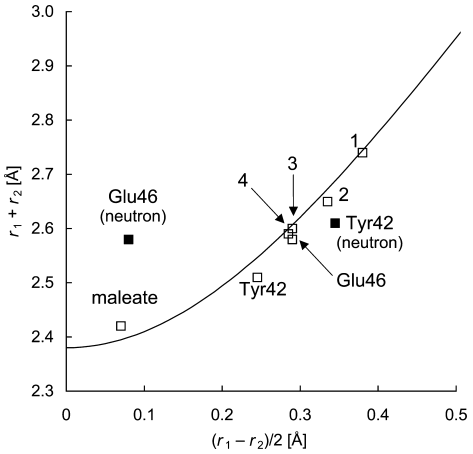

Figure 3. Geometric correlation of the $O_{acceptor}$···H−O_{donor} bond between the acceptor···hydrogen ($O_{acceptor}$···H) distance (r_1) and the donor−hydrogen (O_{donor}−H) distance (r_2) proposed in ref 27: correlation curve (—, eq 1[27]), calculated geometry (□), and neutron diffraction geometry (■). Note that only eq 1 was used to depict the correlation curve (independent of the calculated or neutron diffraction geometries).

bonds and found them to be 14.5 and 14.6 ppm (PDB entry 2ZOH[8]) or 14.6 and 14.0 ppm (PDB entry 1OTB[20]), respectively; these values differ by 0.6−0.7 and 0.3−0.9 ppm from the experimental values of 15.2 and 13.7 ppm,[9] respectively (Table 2). The discrepancy may also reflect the distribution of

Table 2. Experimental[9] and Calculated Values of δ_H (parts per million) for Short H Bonds in PYP (Figure 1)[a]

		calcd δ_H		
	exptl δ_H	QM/MM (2ZOH)	QM/MM (1OTB)	neutron (2ZOI)
Glu46	15.2	14.5	14.6	19.7
(O_{Glu}−O_{pCA})		(2.57)	(2.58)	(2.57)
(O_{Glu}−H)		(1.00)	(1.02)	(1.21)
(H−O_{pCA})		(1.58)	(1.57)	(1.37)
Tyr42	13.7	14.6	14.0	10.2
(O_{Tyr}−O_{pCA})		(2.50)	(2.51)	(2.52)
(O_{Tyr}−H)		(1.01)	(1.01)	(0.96)
(H−O_{pCA})		(1.50)	(1.51)	(1.65)

[a]Distances[14] are in angstroms. The neutron diffraction geometry (PDB entry 2ZOI) was optimized independently by (i) fixing the heavy atom positions and the two H atoms in the O_{Tyr42}−O_{pCA} and O_{Glu46}−O_{pCA} bonds or (ii) fixing only the O_{Tyr42}−H−O_{pCA} and O_{Glu46}−H−O_{pCA} lengths. The two cases resulted in identical chemical shifts.

H bond lengths, even in these high-resolution crystal structures of PYP at resolutions of ∼1 Å (reviewed in ref 20).

We analyzed the δ_H dependence on the H atom position (Figure 4). The origin of downfield character for the chemical shift is considered with respect to the attenuation of the electronic shielding around the proton because of the two electronegative donor and acceptor atoms.[31] The maximal δ_H value of ∼20 ppm was observed near the center of the O_{Glu46}−O_{pCA} bond (Figure 3a). The δ_H of ∼15 ppm measured in solution ^{1}H NMR studies of PYP[9] cannot be obtained near the center of the O_{Glu46}−O_{pCA} bond but only at the Glu46 or *p*CA moiety (Figure 4a). The same tendency holds true for the O_{Tyr42}−O_{pCA} bond (Figure 4b).

In addition, we also analyzed the dependence of δ_H (O_{Glu46}−O_{pCA}) on the lengths of O_{Glu46}−O_{pCA} and O_{Tyr42}−O_{pCA}

dx.doi.org/10.1021/bi201877e | *Biochemistry* 2012, 51, 1171−1177

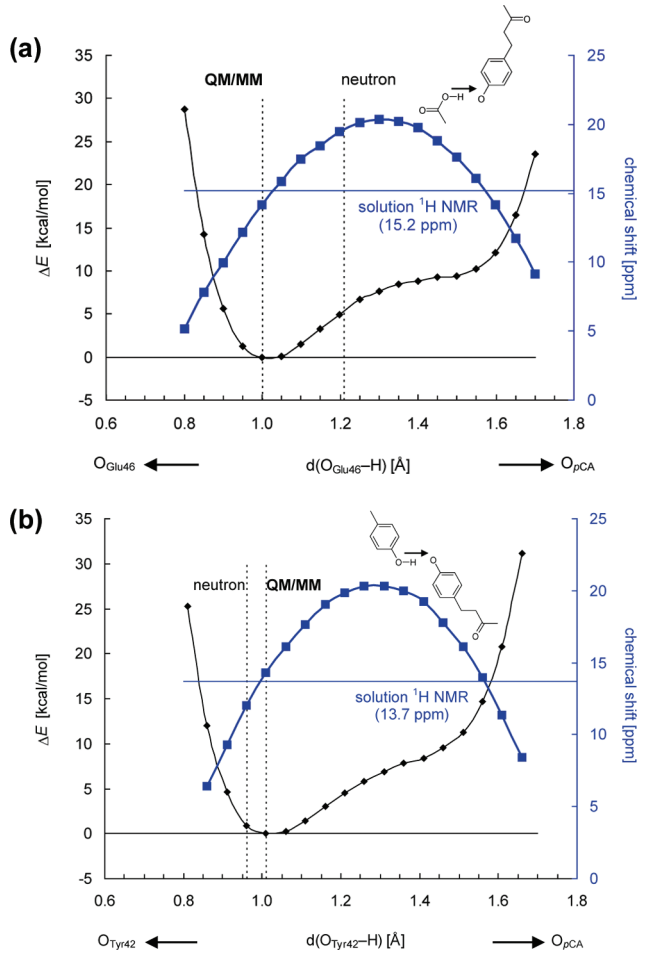

Figure 4. Calculated δ_H (right vertical axis, thick blue line) in parts per million and ΔE (left vertical axis, black line[14]) in kilocalories per mole along the proton transfer coordinate for H bond (a) Glu46–*p*CA and (b) Tyr42–*p*CA donor–acceptor pairs in the PYP protein environment. ΔE describes the difference in energy relative to the energy minimum. The horizontal blue line indicates the δ_H obtained in solution ^{1}H NMR studies.[9] There is no energy minimum near 1.21 Å (neutron diffraction geometry[8]) from O_{Glu46}, and the energy is ~5 kcal/mol higher than that at 1.00 Å (QM/MM geometry[14]). Note that ~5 kcal/mol corresponds to ~3 pK_a units, a non-negligible energy barrier for proton migration. At each point along the proton transfer coordinate, the geometry of the entire QM region except for the focusing H atom was fully optimized at the B3LYP/LACV3P**+ level.

bonds (Figure 5). As the length of the O_{Tyr42}–O_{pCA} bond increased, δ_H for the O_{Glu46}–O_{pCA} bond increased only marginally. The longer O_{Tyr42}–O_{pCA} bond results in the weaker influence of protonated Tyr42 on ionized *p*CA, leading to the pK_a(*p*CA) upshift. The pK_a(*p*CA) upshift that arose from the O_{Tyr42}–O_{pCA} bond, favoring less ionization of *p*CA, causes an increased extent of proton migration from the Glu46 moiety in the O_{Glu46}–O_{pCA} bond, which can increase the calculated δ_H for the O_{Glu46}–O_{pCA} the O_{Glu46}–O_{pCA} bond. Thus, the change in the length of the bond could affect the δ_H for the O_{Glu46}–O_{pCA} bond. Nevertheless, the influence is apparently too weak to increase the δ_H for the O_{Glu46}–O_{pCA} bond to 17–19 ppm, typical δ_H values for LBHBs.[18]

On the other hand, the H atom positions (lengths) of the neutron diffraction study[8] yielded δ_H values of 19.7 and 10.2 ppm for the O_{Glu46}–O_{pCA} and O_{Tyr42}–O_{pCA} bonds, respectively (Table 2). The obtained δ_H value of 19.7 ppm satisfies the criterion of

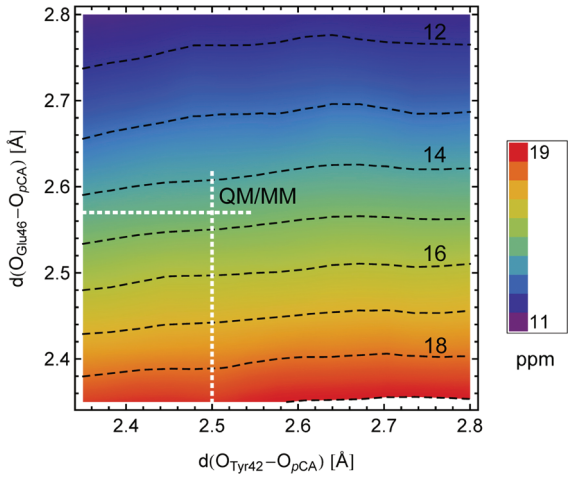

Figure 5. Dependence of the calculated δ_H for the Glu46–*p*CA pair on the lengths of the O_{Glu46}–O_{pCA} and O_{Tyr42}–O_{pCA} bonds. Dotted white lines indicate the QM/MM-optimized bond length of the Glu46–*p*CA pair (see Table 2).

LBHB proposed by Frey (δ_H of 17–19 ppm[18]). The fact that the position of the H atom near the midpoint of the O_{Glu46}–O_{pCA} bond resulted in a δ_H of 19.7 ppm for a typical LBHB[18] is also a clear validation of the criterion proposed by Schutz and Warshel;[12] i.e., the minimum of the potential energy curve in an LBHB is at the center of the O_{Glu46}–O_{pCA} bond. However, a δ_H of 19.7 ppm is obviously larger than the value of 15.2 ppm obtained in NMR studies.[9] Furthermore, the presence of "LBHB" character in the O_{Glu46}–O_{pCA} bond appears, in turn, to significantly decrease the δ_H for the O_{Tyr42}–O_{pCA} bond to 10.2 ppm relative to the experimental value of 13.7 ppm (Table 2). Hence, the H atom positions obtained in the neutron diffraction study[8] result in overestimation of the chemical shift for the O_{Glu46}–O_{pCA} bond and underestimation of that for the O_{Tyr42}–O_{pCA} bond.

Notably, Steiner[29] and Limbach et al.[27] proposed the correlation between δ_H and the H bond geometry; δ_H could be reproduced solely from $(r_1 - r_2)/2$ (or alternatively $r_1 + r_2$), using eqs 1 and 2. The calculated δ_H values were in agreement with the values estimated from the proposed correlation curve,[27] demonstrating that δ_H can be reproduced if a reasonable H bond geometry is provided (Figure 6). From the δ_H correlation curve, the r_1 of 1.37 Å and the r_2 of 1.21 Å reported for the O_{Glu46}–O_{pCA} bond in the neutron diffraction study[8] (Table 2) yielded a δ_H of 20.2 ppm (Figure 6). Thus, a δ_H of ~20 ppm is an inevitable fate of an H atom at the midpoint of the O_{Glu46}–O_{pCA} bond. It should be noted that none of the H bond geometries investigated (even maleate) possessed an H atom at the center of the O–O bond (Figure 6), as previously clarified by Perrin et al.[32,33] This is why two independent approaches (i.e., the correlation proposed by Limbach et al.[27] and QM/MM calculations) reasonably reproduced δ_H values for all of the molecules (11–22 ppm). If an H atom were truly centered between the two O atoms, all of the molecules listed in Tables 1 and 2 would have possessed δ_H values of ~20 ppm.

Proposed Roles of LBHBs in the Function of PYP. The catalytic power of enzymes is due to the stabilization of the transition state relative to bulk water.[34] Thus, H bonds in the catalytic site play an important role in the stabilization of the transition state. An LBHB was originally proposed to possess covalent bond-like character, thus significantly stabilizing the

dx.doi.org/10.1021/bi201877e | *Biochemistry* 2012, 51, 1171–1177

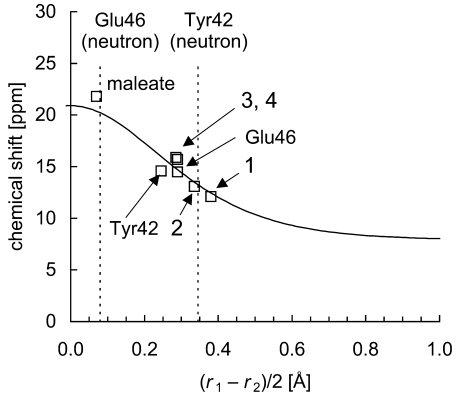

Figure 6. Calculated δ_H values (vertical axis) in parts per million and the $(O_{acceptor}\cdots H)/(O_{donor}-H)$ difference (horizontal axis) in angstroms. r_1 is the $O_{acceptor}\cdots H$ distance and r_2 the $O_{donor}-H$ distance: correlation curve (—, eqs 1 and 2[27]), calculated geometry (□), and neutron diffraction geometry (■). Vertical dotted lines indicate the $(r_1 - r_1)/2$ values of $O_{Glu46}-O_{pCA}$ and $O_{Tyr42}-O_{pCA}$ bonds in the neutron diffraction geometry.[8] Note that only eqs 1 and 2 were used to depict the correlation curve (independent of the calculated geometries).

transition state and facilitating enzymatic reactions.[10,11] In such a covalent bond-like H bond, atomic charges of the H bond donor and acceptor moieties will be more delocalized than those of a conventional H bond. An advantage of the catalytic site of the protein over bulk water is the availability of the preorganized dipoles in the protein environment, stabilizing the transition state electrostatically (e.g., not only polar or charged side chains but also protein backbones). To utilize the protein dipoles effectively, a larger polarity between the transition state and the protein is energetically advantageous. If the H bond is an LBHB (i.e., low polarity), it will lose the electrostatic advantages because of its more delocalized atomic charges.[12,34] In the neutron diffraction studies,[8] it was also proposed that ionized *p*CA was energetically unstable in the hydrophobic chromophore unless the $O_{Glu46}-O_{pCA}$ bond was an LBHB like a covalent bond. As support for the LBHB, deprotonated Arg52 (Figure 1) on the PYP protein bulk surface was presented.[8] However, the conclusion that Arg52 on the PYP protein surface was deprotonated in ref 8 is highly questionable[14] (discussed later).

It was also proposed that the LBHB might facilitate the transfer of a proton from Glu46 to *p*CA in the excited state.[8] However, a widely accepted view is that the proton transfer does not occur in the excited state P* but in the following intermediate states between pR (~3 ns after P*,[35] with protonated Glu46[13]) and pB (with deprotonated Glu46[13]), i.e., pG → P* −(700 fs/7 ps) → I_0 −(220 ps) → $I_0^{\ddagger}$ −(3 ns) → pR − (proton transfer, 250 μs/1.2 ms) → pB −(150 ms/2 s) → pG.[35]

Alternatively, the contribution of the LBHB to "fast proton transfer in the excited state" proposed in ref 8 might correspond to changes in the electronic structures of the *p*CA–Glu46 moiety upon formation of P* rather than the proton transfer in the transition between pR and pB. It was proposed that (i) upon electronic excitation, the $O_{Glu46}-O_{pCA}$ LBHB might be relaxed to a standard H bond and (ii) an H atom might be transferred from the center of the $O_{Glu46}-O_{pCA}$ bond to the Glu46 moiety during the lifetime of the excited state (~1 ps).[8] In ref 8, changes in the CO stretching mode of Glu46 upon formation of P* observed in ultrafast infrared spectroscopic studies[36] were interpreted as an implication of the proton transfer process in the electronic excited state. However, one of the key findings in the ultrafast infrared spectroscopic studies was that the H bond strength of the $O_{Glu46}-O_{pCA}$ bond did not play a crucial role in the transition of the initial part of the PYP photocycle (including the photoinduced *trans–cis* isomerization process of the *p*CA region), as clearly stated in ref 36; mutation of Glu46 to Asn (i.e., the weaker H bond donor) did not essentially alter the kinetics or product yields of the pG to pR transition via P*.[36] Hence, it appears that there is no basis of an LBHB in the PYP ground state contributing to fast proton transfer in the excited state.[8]

■ CONCLUSIONS

Although one might possibly argue that comparison between the solution NMR data[9] and the calculated δ_H values (solid state crystal structure) is not relevant, one also should not ignore the resulting sufficiently high correlation between the two properties (Table 1). Even if the uncertainty of the maximal value of ~1 ppm between measured and calculated δ_H values (Table 1) is considered, the δ_H of 14.5–14.6 ppm obtained in the H atom position of the QM/MM geometries is reasonably closer to the δ_H of 15.2 ppm obtained in the NMR studies than the δ_H of 19.7 ppm obtained in the H atom position of the neutron diffraction studies (Table 2).

The assignment of H atom positions in the neutron diffraction studies should be considered to be essentially reasonable (at 1.5 Å resolution[8]). However, it should also be noted that there are still uncertainties in the conclusion about the presence or absence of an H atom stated in ref 8. In particular, the conclusion about the protonation state of Arg52 on the PYP protein surface being deprotonated in ref 8 is highly questionable. Because in general, not all of the H or D atoms can be assigned in neutron diffraction studies, to conclude a residue is deprotonated requires further careful survey in contrast to the case with a protonated residue. In this respect, the authors of ref 8 did not provide any reasonable explanation of how the existence of deprotonated Arg52 is energetically possible on a protein surface where sufficient solvation energy is available. Furthermore, the nearest positively charged residue, Lys60, is >7 Å from Arg52. In contrast, QM/MM geometries resulted in a significantly smaller root-mean-square deviation with protonated Arg52 (0.14 Å) than with deprotonated Arg52 (0.35 Å) relative to the original crystal structure.[14]

In the previous study,[14] we reported that (i) the potential energy profiles of the $O_{Glu46}-O_{pCA}$ and $O_{Tyr42}-O_{pCA}$ bonds resembled those of standard "asymmetric double-well potentials"[33,37], which differ from those of LBHBs, and (ii) Glu46 was protonated and *p*CA deprotonated as suggested in a number of previous studies;[3−5,13] LBHBs can form only when the pK_a difference between donor and acceptor moieties is nearly zero.[10−12] Thus, the properties of the H bond between Glu46 and *p*CA in the PYP ground state are in contrast to those of the short H bond between D1-Tyr161 (Y_Z) and D1-His190 ($O_{YZ}-O_{D1\text{-}His190}$ distance of 2.46 Å) in photosystem II,[38] where we previously observed a symmetric single-well potential (i.e., ionic H bond[37]) because of the similar pK_a values of the two residues in the protein environment.[39]

In the study presented here, we evaluate the position of an H atom in the $O_{Glu46}-O_{pCA}$ bond on the basis of the calculated chemical shift. A δ_H of 15.2 ppm for the $O_{Glu46}-O_{pCA}$ bond in NMR studies[9] should correspond to the QM/MM geometry (δ_H = 14.5 ppm), where the H atom belongs to the Glu moiety,[14] rather than the neutron diffraction geometry (δ_H = 19.7 ppm),

dx.doi.org/10.1021/bi201877e | *Biochemistry* 2012, 51, 1171–1177

where the H atom is near the midpoint of the donor and acceptor atoms.[8] In addition, according to Frey's definition,[18] a δ_H of 15.2 ppm obtained in the ^{1}H NMR studies[9] is too small for an LBHB (17−19 ppm[18]). Again, the chemical properties of the O_{Glu46}−O_{pCA} bond can be simply explained as a conventional H bond, without invoking the LBHB concept.

■ ASSOCIATED CONTENT

Supporting Information

QM/MM-optimized geometry and charges for PYP and atomic coordinates for compounds listed in Table 1. This material is available free of charge via the Internet at http://pubs.acs.org.

■ AUTHOR INFORMATION

Corresponding Author

*Address: 202 Building E, Career-Path Promotion Unit for Young Life Scientists, Graduate School of Medicine, Kyoto University, Yoshida-Konoe-cho, Sakyo-ku, Kyoto 606-8501, Japan. Telephone: +81-75-753-9286. Fax: +81-75-753-9286. E-mail: hiro@cp.kyoto-u.ac.jp.

Funding

This research was supported by the JST PRESTO program (H.I.), a Grant-in-Aid for Scientific Research from the Ministry of Education, Culture, Sports, Science and Technology (MEXT) of Japan (21770163 to H.I. and 22740276 to K.S.), the Special Coordination Fund (H.I.) for Promoting Science and Technology of MEXT, the Takeda Science Foundation (H.I.), a Kyoto University Step-up Grant-in-Aid for young scientists (H.I.), and a Grant for Basic Science Research Projects from The Sumitomo Foundation (H.I.).

Notes

The authors declare no competing financial interest.

■ ACKNOWLEDGMENTS

We thank Dr. Toyokazu Ishida for valuable discussions.

■ ABBREVIATIONS

δ_H, ^{1}H NMR chemical shift; LBHB, low-barrier hydrogen bond; *p*CA, *p*-coumaric acid; PYP, photoactive yellow protein; QM/MM, quantum mechanical/molecular mechanical; PDB, Protein Data Bank.

■ REFERENCES

(1) Sprenger, W. W., Hoff, W. D., Armitage, J. P., and Hellingwerf, K. J. (1993) The eubacterium *Ectothiorhodospira halophila* is negatively phototactic, with a wavelength dependence that fits the absorption spectrum of the photoactive yellow protein. *J. Bacteriol. 175*, 3096−3104.

(2) Baca, M., Borgstahl, G. E., Boissinot, M., Burke, P. M., Williams, D. R., Slater, K. A., and Getzoff, E. D. (1994) Complete chemical structure of photoactive yellow protein: Novel thioester-linked 4-hydroxycinnamyl chromophore and photocycle chemistry. *Biochemistry 33*, 14369−14377.

(3) Kim, M., Mathies, R. A., Hoff, W. D., and Hellingwerf, K. J. (1995) Resonance Raman evidence that the thioester-linked 4-hydroxycinnamyl chromophore of photoactive yellow protein is deprotonated. *Biochemistry 34*, 12669−12672.

(4) Xie, A., Hoff, W. D., Kroon, A. R., and Hellingwerf, K. J. (1996) Glu46 donates a proton to the 4-hydroxycinnamate anion chromophore during the photocycle of photoactive yellow protein. *Biochemistry 35*, 14671−14678.

(5) Demchuk, E., Genick, U. K., Woo, T. T., Getzoff, E. D., and Bashford, D. (2000) Protonation states and pH titration in the photocycle of photoactive yellow protein. *Biochemistry 39*, 1100−1113.

(6) Borgstahl, G. E., Williams, D. R., and Getzoff, E. D. (1995) 1.4 Å structure of photoactive yellow protein, a cytosolic photoreceptor: Unusual fold, active site, and chromophore. *Biochemistry 34*, 6278−6287.

(7) Getzoff, E. D., Gutwin, K. N., and Genick, U. K. (2003) Anticipatory active-site motions and chromophore distortion prime photoreceptor PYP for light activation. *Nat. Struct. Biol. 10*, 663−668.

(8) Yamaguchi, S., Kamikubo, H., Kurihara, K., Kuroki, R., Niimura, N., Shimizu, N., Yamazaki, Y., and Kataoka, M. (2009) Low-barrier hydrogen bond in photoactive yellow protein. *Proc. Natl. Acad. Sci. U.S.A. 106*, 440−444.

(9) Sigala, P. A., Tsuchida, M. A., and Herschlag, D. (2009) Hydrogen bond dynamics in the active site of photoactive yellow protein. *Proc. Natl. Acad. Sci. U.S.A. 106*, 9232−9237.

(10) Cleland, W. W., and Kreevoy, M. M. (1994) Low-barrier hydrogen bonds and enzymic catalysis. *Science 264*, 1887−1890.

(11) Frey, P. A., Whitt, S. A., and Tobin, J. B. (1994) A low-barrier hydrogen bond in the catalytic triad of serine proteases. *Science 264*, 1927−1930.

(12) Schutz, C. N., and Warshel, A. (2004) The low barrier hydrogen bond (LBHB) proposal revisited: The case of the Asp...His pair in serine proteases. *Proteins 55*, 711−723.

(13) Kandori, H., Iwata, T., Hendriks, J., Maeda, A., and Hellingwerf, K. J. (2000) Water structural changes involved in the activation process of photoactive yellow protein. *Biochemistry 39*, 7902−7909.

(14) Saito, K., and Ishikita, H. (2012) Energetics of short hydrogen bonds in photoactive yellow protein. *Proc. Natl. Acad. Sci. U.S.A. 109*, 167−172.

(15) Nozaki, Y., and Tanford, C. (1967) Acid-base titrations in concentrated guanidine hydrochloride. Dissociation constants of the guamidinium ion and of some amino acids. *J. Am. Chem. Soc. 89*, 736−742.

(16) Kroon, A. R., Hoff, W. D., Fennema, H. P., Gijzen, J., Koomen, G. J., Verhoeven, J. W., Crielaard, W., and Hellingwerf, K. J. (1996) Spectral tuning, fluorescence, and photoactivity in hybrids of photoactive yellow protein, reconstituted with native or modified chromophores. *J. Biol. Chem. 271*, 31949−31956.

(17) Jeffrey, G. A. (1997) *An Introduction to Hydrogen Bonding*, Oxford University Press, Oxford, U.K.

(18) Frey, P. A. (2006) in *Isotope Effects in Chemistry and Biology* (Kohen, A., and Limbach, H.-H., Eds.) pp 975−993, CRC Press, Boca Raton, FL.

(19) Frey, P. A. (2001) Strong hydrogen bonding in molecules and enzymatic complexes. *Magn. Reson. Chem. 39*, S190−S198.

(20) Anderson, S., Crosson, S., and Moffat, K. (2004) Short hydrogen bonds in photoactive yellow protein. *Acta Crystallogr. D60*, 1008−1016.

(21) Warshel, A., and Levitt, M. (1976) Theoretical studies of enzymic reactions: Dielectric, electrostatic and steric stabilization of the carbonium ion in the reaction of lysozyme. *J. Mol. Biol. 103*, 227−249.

(22) *QSite*, version 5.6 (2010) Schrödinger, LLC, New York.

(23) Cao, Y., Beachy, M. D., Braden, D. A., Morrill, L., Ringnalda, M. N., and Friesner, R. A. (2005) Nuclear-magnetic-resonance shielding constants calculated by pseudospectral methods. *J. Chem. Phys. 122*, 224116.

(24) *Jaguar*, version 7.5 (2008) Schrödinger, LLC, New York.

(25) Wolf, A. K., Glinnemann, J., Fink, L., Alig, E., Bolte, M., and Schmidt, M. U. (2010) Predicted crystal structures of tetramethylsilane and tetramethylgermane and an experimental low-temperature structure of tetramethylsilane. *Acta Crystallogr. B66*, 229−236.

(26) Kamerlin, S. C., Haranczyk, M., and Warshel, A. (2009) Progress in *ab initio* QM/MM free-energy simulations of electrostatic energies in proteins: Accelerated QM/MM studies of pK_a, redox reactions and solvation free energies. *J. Phys. Chem. B 113*, 1253−1272.

(27) Limbach, H.-H., Tolstoy, P. M., Pérez-Hernández, N., Guo, J., Shenderovich, I. G., and Denisov, G. S. (2009) OHO hydrogen bond geometries and NMR chemical shifts: From equilibrium structures to

geometric H/D isotope effects, with applications for water, protonated water, and compressed ice. *Isr. J. Chem. 49*, 199−216.
(28) Hibbert, F., and Emsley, J. (1990) Hydrogen bonding and chemical reactivity. *Adv. Phys. Org. Chem. 26*, 255−379.
(29) Steiner, T. (1998) Lengthening of the covalent X−H bond in heteronuclear hydrogen bonds quantified from organic and organometallic neutron crystal structures. *J. Phys. Chem. A 102*, 7041−7052.
(30) Koeppe, B., Tolstoy, P. M., and Limbach, H. H. (2011) Reaction pathways of proton transfer in hydrogen-bonded phenol-carboxylate complexes explored by combined UV-vis and NMR spectroscopy. *J. Am. Chem. Soc. 133*, 7897−7908.
(31) Ishida, T. (2006) Low-barrier hydrogen bond hypothesis in the catalytic triad residue of serine proteases: Correlation between structural rearrangement and chemical shifts in the acylation process. *Biochemistry 45*, 5413−5420.
(32) Perrin, C. L., and Thoburn, J. D. (1992) Symmetries of hydrogen bonds in monoanions of dicarboxylic acids. *J. Am. Chem. Soc. 114*, 8559−8565.
(33) Perrin, C. L. (2010) Are short, low-barrier hydrogen bonds unusually strong? *Acc. Chem. Res. 43*, 1550−1557.
(34) Warshel, A., and Papazyan, A. (1996) Energy considerations show that low-barrier hydrogen bonds do not offer a catalytic advantage over ordinary hydrogen bonds. *Proc. Natl. Acad. Sci. U.S.A. 93*, 13665−13670.
(35) Ihee, H., Rajagopal, S., Srajer, V., Pahl, R., Anderson, S., Schmidt, M., Schotte, F., Anfinrud, P. A., Wulff, M., and Moffat, K. (2005) Visualizing reaction pathways in photoactive yellow protein from nanoseconds to seconds. *Proc. Natl. Acad. Sci. U.S.A. 102*, 7145−7150.
(36) van Wilderen, L. J., van der Horst, M. A., van Stokkum, I. H., Hellingwerf, K. J., van Grondelle, R., and Groot, M. L. (2006) Ultrafast infrared spectroscopy reveals a key step for successful entry into the photocycle for photoactive yellow protein. *Proc. Natl. Acad. Sci. U.S.A. 103*, 15050−15055.
(37) Perrin, C. L., and Nielson, J. B. (1997) "Strong" hydrogen bonds in chemistry and biology. *Annu. Rev. Phys. Chem. 48*, 511−544.
(38) Umena, Y., Kawakami, K., Shen, J.-R., and Kamiya, N. (2011) Crystal structure of oxygen-evolving photosystem II at 1.9 Å resolution. *Nature 473*, 55−60.
(39) Saito, K., Shen, J.-R., Ishida, T., and Ishikita, H. (2011) Short hydrogen-bond between redox-active tyrosine Y_Z and D1-His190 in the photosystem II crystal structure. *Biochemistry 50*, 9836−9844.